



ELSEVIER

Available online at www.sciencedirect.com

SCIENCE @ DIRECT®

Journal of Crystal Growth 268 (2004) 494–498

JOURNAL OF
**CRYSTAL
GROWTH**

www.elsevier.com/locate/jcrysgro

Depth-resolved luminescence imaging of epitaxial lateral overgrown GaN using ionoluminescence

E.J. Teo^{a,*}, A.A. Bettiol^a, T. Osipowicz^a, M. Hao^b, S.J. Chua^b, Y.Y. Liu^c

^a Centre for Ion Beam Applications, Department of Physics, National University of Singapore, 2 Science Drive 3, Singapore 117542, Singapore

^b Institute of Materials Research and Engineering, National University of Singapore, Singapore 119260, Singapore

^c Centre for Integrated Circuit Failure Analysis and Reliability, Department of Electrical and Electronic Engineering, National University of Singapore, Singapore 119260, Singapore

Abstract

In this article, we utilize energetic mega-electron-volt (MeV) H^+ to excite light emission from epitaxial lateral overgrown GaN. Due to the high-penetration depth of MeV ions, this technique allows us to probe several microns below the surface, down to the interface region. Spatially and depth-resolved yellow luminescence imaging is carried out using a focused H^+ beam with energies of 0.5, 0.75 and 1 MeV. Results show an increase of the yellow luminescence with depth in the window regions with respect to the wing regions. Since the threading dislocations propagate to the surface, this suggests that the yellow luminescence is due to the point defects rather than threading dislocations.

© 2004 Elsevier B.V. All rights reserved.

PACS: 78.60.Hk; 29.17.+w; 81.05.Ea; 61.72.Hh

Keywords: A1. Cathodoluminescence; A1. Depth-resolved; A1. Ionoluminescence; B1. Epitaxial lateral overgrown GaN

1. Introduction

Due to its importance in optoelectronic applications, the luminescence properties of GaN have been studied extensively with various techniques such as photoluminescence (PL) and cathodoluminescence (CL). In addition to the near band edge emission, a defect-related yellow band is often observed in as-grown GaN. Many groups have

performed CL measurements to investigate the correlation of yellow luminescence (YL) with extended defects [1,2]. However, analysis using these techniques is limited to near surface regions and may not represent bulk material properties. This restricts the understanding of the defect-related yellow luminescence in GaN, since dislocations and defects tends to originate at the interface region as a consequence of the lattice mismatch between the layer and substrate. In order to reveal features not detectable in planar view, some groups have carried out CL measurements in cross-sectional view [3]. We propose the utilization

*Corresponding author. Tel.: +65-6874-4136; fax: 65-6777-6126.

E-mail address: phytej@nus.edu.sg (E.J. Teo).

of a focused MeV H^+ beam to probe several microns into the GaN layer with ion-induced luminescence or ionoluminescence (IL) technique. Monte Carlo simulations of the ionization profile show that MeV ions have a much higher penetration depth than the keV electrons used in CL. By making use of the well-defined electronic energy loss peak or ‘Bragg peak’ at the end of range, depth-resolved imaging of the YL distribution can be performed. The small lateral spreading of a MeV H^+ ion in the material also enables high-resolution imaging of buried defects in GaN.

In this work, MeV H^+ ions with different energies are employed to investigate the change of the YL distribution in epitaxial lateral overgrown (ELO) GaN layer with depth. The spatial distribution of the threading dislocations in ELO GaN also allows for the investigation of the correlation of threading dislocations with YL.

2. Experimental details

Lateral overgrown GaN stripes, patterned by the underlying Si_3N_4 mask, were deposited on GaN buffer layer/ [0001] Al_2O_3 substrate. Initially, a 2 μm thick GaN seed layer was grown along [1 $\bar{1}$ 0 0] by MOCVD (40 min) on a *c*-plane sapphire substrate. A 100 nm SiN mask layer was deposited on GaN by plasma enhanced chemical vapor deposition (PECVD) and then patterned into oriented stripes, which define a 3 μm opening (window) at a periodicity of 13 μm . The lateral overgrowth GaN layer was achieved at a pressure of 100 Torr, with trimethylgallium (TMG) and NH_3 at a flow rate of 123 $\mu mol/min$ and 10,000 sccm, respectively, in combination with 6000 sccm of H_2 diluent. After the regrowth of the GaN, stripes of 8 μm thickness propagated vertically through the window, with a width of 12.8 μm over the mask so that the stripes are close to coalescence.

Various depths of the ELO GaN are probed using H^+ ions with energies of 1.0, 0.75 and 0.5 MeV produced at the Singletron accelerator facility at the National University of Singapore [4]. The ion beam is focused on to a sub-micron spot size with three magnetic quadruple lens and

scanned across the sample. Light emission induced by the ions is then detected by a Hamamatsu H7421-40 Single Photon Counting Head via a Perspex light pipe. For YL monochromatic imaging, an interference notch filter with a transmission wavelength of 550 nm is placed in front of the PMT. The high sensitivity of the PMT enables the collection of the IL image with a typical beam current of less than 1 pA. This helps limit the ion beam damage on the sample.

For comparison, CL measurements using 25 keV electrons are also performed on the same sample using an SEM system. The CL signals are collected with a semi-ellipsoidal mirror and coupled into the Hamamatsu R928 PMT via a bundle of optical fibers. A JOBIN YVON model H10-IR monochromator is used for monochromatic imaging and spectral analysis. Monte Carlo simulations of the electronic energy loss profile of electrons and ions have also been carried out using the software packages CASINO [5] and SRIM 2000 [6], respectively. All IL and CL measurements are collected at room temperature.

3. Results

IL is an analogous imaging technique to CL where the light generation mechanism is governed by the electronic energy loss of the ions or electrons in the material. The main difference between the two techniques lies in the generation volume, which is basically determined by the range and lateral spreading of the beam. Fig. 1 shows the SRIM simulation for the ionization profile of different H^+ energies in GaN. The electronic energy loss profile of 25 keV electrons is plotted on the same graph for comparison, using the CASINO software. The ionization profile is proportional to the number of e–h pairs created as the beam traverses into the material. It can be seen that the electronic energy loss for 25 keV incident electrons is about 2 orders of magnitude smaller than that for MeV H^+ ions. Therefore, for 1.0 MeV H^+ , the total number of e–h pairs created is 40 times larger than that produced by a 25 keV electron.

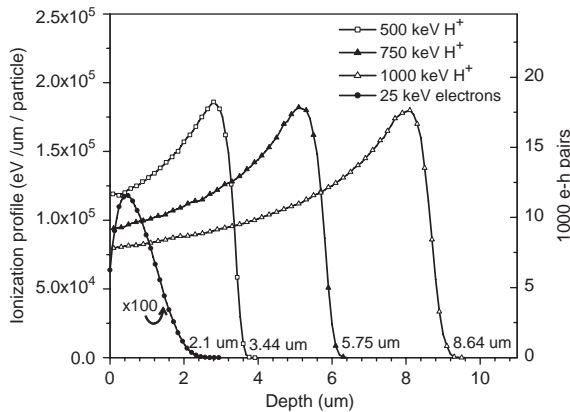


Fig. 1. Ionization profile of 1.0, 0.75 and 0.5 MeV H^+ ions simulated using SRIM2000. This is compared with that of 25 keV electrons simulated using CASINO software. The number of e-h pairs created is proportional to the ionization profile.

Most of the ionization for 25 keV electrons occurs in the first $0.5 \mu\text{m}$ below the surface, while $1 \text{ MeV } H^+$ ions suffer most electronic energy loss at the end of range and at a much longer penetration depth. This well-defined peak known as the ‘Bragg’ peak allows us to measure depth-resolved information of the YL in the sample, provided that the absorption of the light is negligible in the material [7]. Since GaN is transparent to yellow light, we have assumed that the absorption of YL in GaN is negligible. By increasing the H^+ energy from 0.5 to 1.0 MeV, the penetration depth is increased from 3.4 to $8.6 \mu\text{m}$. This depth range probes the interface region between the GaN overgrown and seed layer.

Fig. 2 shows the lateral spreading of keV electron and MeV ion in GaN. It can be seen that keV electrons spread out spherically while the energetic ion has a more well-defined path and range in the material. Since the diffusion length of the e-h pairs in GaN is only about 50–100 nm [8,9], the spatial resolution is mainly determined by the lateral spreading of the beam. Simulations show that 1.0 MeV H^+ ions has a comparable lateral spread to 25 keV electrons. This indicates that MeV H^+ ions are suitable for depth profiling of buried defects, without suffering significant loss of spatial resolution with depth. The correspond-

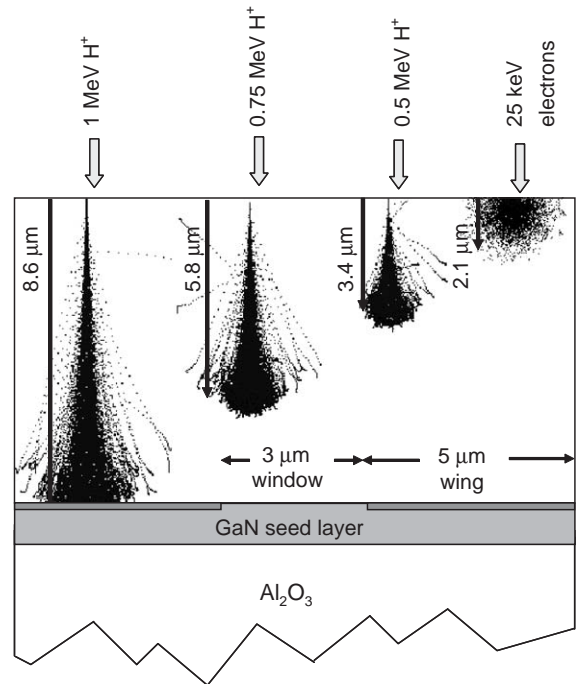


Fig. 2. Simulation of the generation volume and range for 1.0, 0.75, 0.5 MeV H^+ and 25 keV electrons in the ELO GaN sample.

ing regions of interest probed by the different energies proton beams in the ELO GaN sample are shown and compared with those of 25 keV electron beam.

Fig. 3(a) shows the planar view of the surface morphology of the nearly-coalescent ELO GaN sample. The GaN stripes are $13 \mu\text{m}$ in width and the gap between the stripes is the coalescent front. The corresponding UV image of the same region is shown in Fig. 3(b). It can be clearly seen that the $3 \mu\text{m}$ wide window regions of the ELO GaN has a much lower UV emission as compared to the wing regions. This shows that the threading dislocations in the window regions act to quench the UV luminescence. Individual point spectra are extracted from the window and wing regions and plotted in Fig. 3(c). The UV intensity is about 3 times higher in the good crystalline wing regions than the window regions. The yellow bands in the wing and window regions do not show any difference in intensity at this depth.

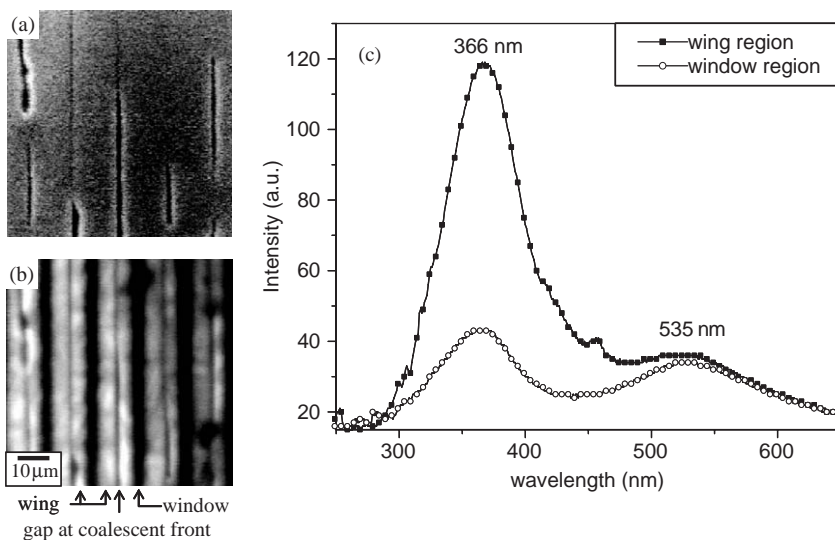


Fig. 3. (a) SEM micrograph showing the planar view of the ELO GaN sample. (b) Corresponding UV image of the same region. (c) Individual point spectra collected from the wing and window region.

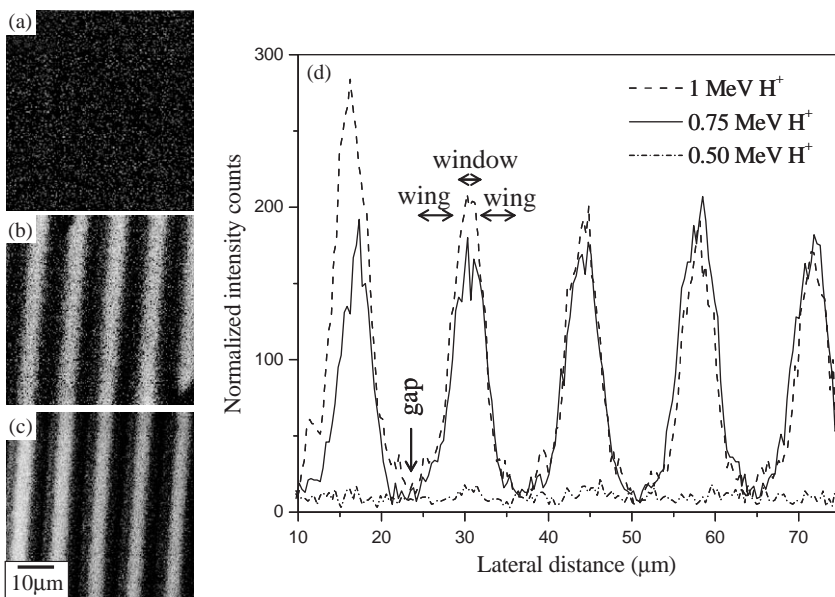


Fig. 4. YL map collected at (a) 3.4 μm , (b) 5.8 μm and (c) 8.6 μm with 0.5, 0.75 and 1 MeV H^+ beam, respectively. (d) Line profiles of the yellow intensity across the GaN stripes at three different depths.

Figs. 4(a)–(c) show the YL maps collected at 3.4, 5.8 and 8.6 μm below the surface. At a depth of 3.4 μm , the YL intensity is relatively low and it is homogeneously distributed across the GaN stripes. When the probing depth increased to

5.8 μm , the yellow intensity starts to increase at the window regions, while the wing regions still remain low in intensity. The window regions appear distinctively higher in yellow intensity with respect to the wing regions at the interface region

of 8.6 μm below the surface. Dark lines seen in the high-resolution YL map correspond to the gaps between adjacent overgrown GaN stripes that are close to coalescence. Fig. 4(d) shows the line profiles of the YL intensity extracted at different depths of the ELO GaN sample. The intensity in the window region is about five times higher than that observed in the wing region at a depth of 5.8 and 8.6 μm below the surface. Since the threading dislocations propagate to the surface (published previously in Ref. [10]), this suggests that threading dislocations are not the origin of the YL and point defects are more likely candidate for the mid-band gap transition. The higher yellow luminescence observed at the window regions with depth could be due to the diffusion of the point defects from the seed layer to the overgrown layer [11].

4. Conclusions

CL and IL imaging of ELO GaN show that IL is a more suitable technique for depth profiling of YL due to the much higher probing depth and smaller lateral beam spreading in the material. It is found that there is a strong dependence of YL distribution with depth. The yellow intensity is low and homogeneously distributed across the GaN stripes for regions near the surface. As the probing depth increases, the YL intensity starts to increase in the window regions with respect to the wing regions. This suggests that YL is not due to

threading dislocations since they propagate to the surface in the window regions. These results demonstrated the importance of depth profiling with IL to provide a better understanding of the origin of YL.

References

- [1] Z. Yu, M.A.L. Johnson, T. McNulty, J.D. Brown, J.W. Cook Jr., J.F. Schetzina, MRS Internet J. Nitride Semicond. Res. 3 (1998) 6.
- [2] S. Dassonneville, A. Amokrane, B. Sieber, J.-L. Farvacque, B. Beaumont, P. Gilbart, J. Appl. Phys. 89 (7) (2001) 3736.
- [3] M.H. Zaldivar, P. Fernandez, J. Piqueras, J. Appl. Phys. 83 (5) (1998) 2796.
- [4] D.J.W. Mous, R.G. Haitisma, T. Butz, R.H. Flagmeyer, D. Lehmann, J. Vogt, Nucl. Instrum. and Meth. Phys. Res. B 130 (1997) 31.
- [5] P. Hovington, D. Drouin, R. Gauvin, Scanning 19 (1997) 1. <http://www.gel.usherb.ca/casino/>.
- [6] J.F. Ziegler, J.P. Biersack, SRIM2000 v0.09—The stopping and range of ions in solids, IBM, 1998. <http://www.srim.org/>.
- [7] K. Klobloch, P. Perlin, J. Krueger, E.R. Weber, C. Kisielowski, MRS Internet J. Nitride Semicond. Res. 3 (1998) 4.
- [8] S. Chichibu, T. Azuhata, T. Soto, S. Nakamura, Appl. Phys. Lett. 70 (1997) 2822.
- [9] S. Nakamura, Science 281 (1998) 956.
- [10] M. Hao, W. Wang, P. Li, W. Liu, S.J. Chua, Proceedings of the International Workshop on Nitride Semiconductors (IWN2000) Nagoya, Aichi, Japan, IPAP Conference Series 1, 2000, pp. 312.
- [11] G. Popovici, W. Kim, A. Botchkarev, H. Tang, H. Morkoc, J. Solomon, Appl. Phys. Lett. 71 (23) (1997) 3385.